Published in final edited form as:
Nat Ecol Evol. 2018 May ; 2(5): 873–881. doi:10.1038/s41559-018-0529-z.

Multicopy plasmids allow bacteria to escape from fitness trade-offs during evolutionary innovation

Jeronimo Rodriguez-Beltran[a,*], **J. Carlos R. Hernandez-Beltran**[b], **Javier DelaFuente**[a], **Jose A. Escudero**[c], **Ayari Fuentes-Hernandez**[b], **R. Craig MacLean**[d], **Rafael Peña-Miller**[b], and **Alvaro San Millan**[a,e,*]

[a]Department of Microbiology, Hospital Universitario Ramon y Cajal (IRYCIS), 28034 Madrid, Spain

[b]Centro de Ciencias Genómicas, Universidad Nacional Autónoma de México, 62210, Morelos, Mexico

[c]Departamento de Sanidad Animal and VISAVET, Facultad de Veterinaria, Universidad Complutense de Madrid, 28040, Madrid. Spain

[d]Department of Zoology, University of Oxford, Oxford OX2 6GG, UK

[e]Network Research Center for Epidemiology and Public Health (CIBER-ESP), Madrid, Spain

Abstract

Understanding the mechanisms governing innovation is a central element of evolutionary theory. Novel traits usually arise through mutations in existing genes, but trade-offs between new and ancestral protein functions are pervasive and constrain the evolution of innovation. Classical models posit that evolutionary innovation circumvents the constraints imposed by trade-offs through genetic amplifications, which provide functional redundancy. Bacterial multicopy plasmids provide a paradigmatic example of genetic amplification, yet their role in evolutionary innovation remains largely unexplored. Here, we reconstructed the evolution of a new trait encoded in a multicopy plasmid using TEM-1 β-lactamase as a model system. Through a combination of theory and experimentation, we show that multicopy plasmids promote the coexistence of ancestral and novel traits for dozens of generations, allowing bacteria to escape the evolutionary constraints imposed by trade-offs. Our results suggest that multicopy plasmids are excellent platforms for evolutionary innovation, contributing to explain their extreme abundance in bacteria.

[*]**Correspondence and request for materials** should be addressed to Jeronimo Rodriguez-Beltran (jeronimo.rodriguez.beltran@gmail.com) & Alvaro San Millan (alvsanmillan@gmail.com).

Author contributions

J.R.B, A.S.M and R.C.M were responsible for the conceptualization of the study; J.R.B, A.S.M, J.A.E designed the methodology; R.P.M, J.C.R.H.B. and A.F.H. postulated and analyzed the mathematical model; J.C.R.H.B, A.F.H, J.A.E, J.D and J.R.B performed experiments and contributed to data analysis; J.R.B and A.S.M analyzed data and prepared the original draft of the manuscript and undertook the reviewing and editing; All authors supervised and approved the final version of the manuscript. A.S.M was responsible for funding acquisition and supervision.

Competing interests

The authors declare no competing interests.

Europe PMC Funders Author Manuscripts

The ability of a species to expand its ecological niche and thrive in new environments depends directly on the development of novel adaptive traits through evolutionary innovation. Evolutionary innovation, in turn, relies on the repurposing of old traits to serve new roles[1,2]. Examples of this process are abundant and include the development of important traits such as new metabolic capabilities[3], the control of bacterial division[4], and the evolution of multicellularity[5]. However, mutations providing a new role are usually detrimental to native gene function. These negative correlations between ancestral and evolved traits are called trade-offs. Trade-offs are common during evolutionary innovation and have been identified in a plethora of natural and experimental settings[2]. Crucially, the interplay between trade-offs and selective pressures for the ancestral and new activities determines the fate of innovative mutations. For instance, strong selection to maintain the native activity leads to the purging of variants with adaptive potential, hampering innovative evolution[6,7]. Hence, trade-offs are arguably one of the major constraints on evolutionary innovation.

Several models have been proposed to explain the ready occurrence of innovation despite the restraints imposed by trade-offs. Most of these models are based on the emergence of genetic amplifications that provide genetic redundancy[1,8–11]. Amplifications, such as duplications, alleviate trade-offs because they allow the coexistence of different alleles of the same gene. In this way, extra gene copies might acquire new functions while others retain their original role[8]. However, genetic amplifications might be unstable as they are usually a target for homologous recombination, resulting in the deletion of one of the duplicated regions[10,12]. Furthermore, the majority of amplifications have been found to be neutral or deleterious in the absence of selection[13]. Nevertheless, stable amplifications have been reported for genes involved in antibiotic resistance[14], metabolism[15] or encoding weak secondary functions[11,16].

Among the most paradigmatic examples of genetic mechanisms providing genetic redundancy in prokaryotes are multicopy plasmids (MCPs). MCPs are small and highly prevalent genetic elements in bacteria[17], that typically range from 10 to 30 copies per cell and lack active segregation and partition systems[18]. Therefore, MCPs maintain a population of the same genes within a cell, and thus can be regarded as an extreme example of stable genetic amplification. Here, we propose that MCPs could alleviate trade-offs during the evolution of innovation. This hypothesis is based on two predictions. First, the multicopy nature of these plasmids allows different versions of the gene (alleles) to coexist in the same cell under heterozygosity, and this coexistence will alleviate fitness trade-offs. Second, once the evolved allele appears, plasmid segregation and replication dynamics will maintain heterozygosity at the cellular and population level for a prolonged period of time, even under strong selection for one of the alleles (Fig. 1a). To test these predictions, we used a well-characterized model of antibiotic resistance evolution in which trade-offs have profound effects on adaptive trajectories[7,19,20]. By combining simple mathematical models with experimental work, we demonstrate that MCPs promote the maintenance of genetic diversity against strong selection, alleviating trade-offs and promoting evolutionary innovation.

Results

Experimental System

TEM-1 is a β-lactamase that confers high-level resistance to penicillins such as ampicillin (Amp) but negligible resistance to third generation cephalosporins such as ceftazidime (Caz). The evolution of TEM-1 toward conferring Caz resistance has been shown in laboratory and natural settings to occur predominantly via a single mutation (Arg164Ser) that gives rise to TEM-1219,21. The evolved allele ($bla_{\text{TEM-12}}$) confers high-level resistance to Caz at the expense of a reduced activity against Amp compared with the ancestral allele ($bla_{\text{TEM-1}}$), thus demonstrating a trade-off between Amp and Caz resistance19,21. In a recent study, we detected TEM-12 mutation arising in response to Caz pressure in an experimental model using plasmid pBGT-1; a MCP carrying $bla_{\text{TEM-1}}$21. Crucially, sequencing of evolved clones revealed pBGT-1 plasmid variants differing only in the TEM Arg164 residue coexisting under heterozygosity (see Supplementary file 2 of San Millan *et al.*21). To test the ability of MCPs to alleviate trade-offs, we reproduced the TEM-1 evolutionary scenario using a traceable MCP system. We developed two plasmids coding TEM-1 or TEM-12. As the ancestral allele carrier we used plasmid pBGT-1, which occurs at ~19 copies per bacterium and includes a $bla_{\text{TEM-1}}$ gene and a tightly controlled *gfp* gene21. In parallel, we constructed the pBRT-12 plasmid by replacing $bla_{\text{TEM-1}}$ with $bla_{\text{TEM-12}}$ and the *gfp* gene with *dsRed* to allow plasmid identification by fluorescence (Fig. 1b). We also constructed plasmids with interchanged fluorescent markers (pBGT-12 and pBRT-1; Supplementary Fig. 1) and used them to show that the reporter genes did not influence the results obtained hereafter (Supplementary table 1, Supplementary Figs. 2-4). We transformed *Escherichia coli* MG1655 with the pBGT1 and pBRT12 plasmids individually, respectively generating the G1 and R12 strains, and also together to generate a heterozygote strain (HT) carrying both plasmids (Supplementary table 1). Direct observation of cells under confocal microscopy (Fig. 1c) and whole genome sequencing of the genomes of all strains confirmed their isogenic nature and the presence of the different plasmids.

Multicopy plasmid-mediated heterozygosity alleviates trade-offs

It is reasonable to expect that, by maintaining copies of the ancestral and the evolved alleles within individual cells, MCPs would alleviate trade-offs emerging during evolutionary innovation. To test this possibility, we measured the ability of the G1, R12, and HT strains to colonize an array of 48 liquid environments containing varying concentrations of Caz or Amp alone or in combination (Fig. 2a). We also included a 1:1 mixed population of the G1 and R12 homozygotes as a control. The G1 and R12 strains were unable to grow at high concentrations of Caz or Amp, respectively, demonstrating the anticipated trade-off (Fig. 2a). In contrast, both the HT and the mixed population colonized a significantly higher number of antibiotic environments than the ancestral (G1) and evolved (R12) strains (Fig. 2b; One Way ANOVA $F=290.7$, d.f.=3, $P<0.001$ followed by Tukey's multiple comparison of means $P<0.001$). This result indicated that the presence of both alleles, either at the population level (the mixed population) or at the cellular level (the HT strain), allowed bacterial populations to persist in the presence of Caz and Amp.

Because the plasmids used in this study were engineered to carry distinguishable fluorescence reporters (Fig. 1b), we were able to estimate the relative abundance of $bla_{\text{TEM-1}}$ and $bla_{\text{TEM-12}}$ alleles by simply measuring the GFP/RFP ratio in each environment (Methods and Supplementary Fig. 5). As expected, both the HT and the mixed populations – but not the homozygotes– showed variation in the plasmid proportions in every environment in response to different antibiotic combinations (Fig. 2c). In general, higher concentrations of Caz selected for higher proportions of pBRT12, biasing fluorescence toward red (Spearman's rho -0.58 and -0.71 for Mix and HT, respectively; $P<0.01$). Higher Amp concentrations selected for pBGT1, and therefore produced a higher GFP/RFP ratio (Spearman's rho 0.92 and 0.69 for Mix and HT, respectively; $P<0.03$).

To quantify allelic richness across environments, we counted the environments that contained both plasmids at detectable levels (i.e. environments with fluorescence ratios between those of the homozygote populations; shaded region on Fig. 2d). Although the HT and Mix populations were able to colonize the same number of environments, HT maintained both alleles to a greater extent than the mixed population (45% [38/84] versus 23% [18/78] of the colonized environments, respectively; $\chi^2=7.8293$, d.f.=1, $P<0.01$).

Multicopy plasmids maintain genetic diversity against selection

Our second prediction was that once an adaptive mutation appears in a MCP, random plasmid segregation will maintain heterozygosity at the cellular level (and consequently at the population level) for a prolonged period, even under strong selection for one of the alleles. To study the fixation dynamics of the innovative allele $bla_{\text{TEM-12}}$ under strong Caz selective pressure, we performed invasion experiments in which a small (~1%) HT population invades a G1 population. As a control, we performed the same experiment with R12, instead of HT, invading the G1 population (Fig. 3). The experiment, which ran for 8 days with four replicates per treatment, started with the minimal selective concentration22 of Caz for the $bla_{\text{TEM-12}}$ allele (0.0625mg/L; Supplementary Fig. 4). Every day, 0.1% of each population was transferred to fresh medium containing double the Caz concentration of the preceding day. The relative abundance of each genotype was tracked by selective plating, and the frequency of the $bla_{\text{TEM-1}}$ and $bla_{\text{TEM-12}}$ alleles in every population was determined by qPCR.

The results showed that the G1 strain was rapidly outcompeted both by the R12 and HT strains at the same Caz concentration (¼ of the G1 minimal inhibitory concentration; MIC). In the control invasions this meant the rapid fixation of the R12 genotype. However, in the HT invasions, the HT strain displaced G1 but never reached fixation as it was gradually replaced by R12 cells that emerged as segregants through intracellular fixation of pBRT-12. Even so, HT cells were still detectable at the end of the experiment (mean 14.8%; range 0.005-37.9%) after approximately 77 bacterial generations under increasing selective pressure for the $bla_{\text{TEM-12}}$ allele. qPCR results confirmed that $bla_{\text{TEM-1}}$ is maintained throughout the experiment when HT is invading. Interestingly, these results showed that HT cells are able to maintain $bla_{\text{TEM-1}}$ in the population well above the MIC of Caz conferred by this allele, increasing the allelic diversity of these populations throughout the experiment. This result is demonstrated by the fact that the Simpson diversity index calculated from

qPCR data over the experiment is significantly higher when the invading strain is HT than when it is R12 (Repeated-Measures ANOVA invading genotype by time interaction $F_{7,21}$=4.767, P<0.003). Taken together, these results demonstrate that by slowing down the fixation of beneficial mutations multicopy plasmids preserve genetic diversity against strong selective pressures.

Multicopy plasmids promote adaptation under constant and fluctuating selective pressures

We have shown that MCPs allow populations to invade new environmental conditions and maintain genetic diversity over time in bacterial populations. These results suggest that MCPs may provide an important evolutionary advantage by alleviating trade-offs over time and promoting adaptation in bacterial populations under strong selective pressures. To test this possibility, we designed a short-term selection experiment in which we propagated G1, R12, HT, and mixed populations (G1+R12) under constant or fluctuating strong selective pressure with Amp (4,096 mg/l) and Caz (16 mg/l) over a period of two days (see diagram in Fig. 4a). Although below the MIC, these concentrations are the highest at which growth of any of the genotypes was observed and therefore imposed an extremely stringent selective pressure for the bla_{TEM} alleles. This approach led to four possible antibiotic treatment routes that can be grouped into two constant selection regimes (Amp→Amp and Caz→Caz) and two fluctuating selection regimes (Amp→Caz and Caz→Amp). Every day, the populations able to survive the antibiotic treatments were inoculated into a fresh complete array of 48 Caz/Amp environments. With this experiment, we were able to measure two adaptive traits for each genotype: (i) survival under strong selective pressure and (ii) the ability to grow in 48 Caz/Amp environments after selection. We predicted that the HT population would be able to escape trade-offs over time better that any other genotype, leading both to higher survival and to better colonization of Caz/Amp environments after the antibiotic treatments, especially under fluctuating selection regimes.

These predictions were confirmed with four experimental replicates for each genotype and treatment (Fig. 4b and Supplementary Data 1). The extinction patterns showed that while the HT strain was relatively insensitive to the antibiotic treatment, the homozygotes and the mixed populations faced massive extinctions. This pattern was especially true under fluctuating selection regimes, where all G1 replicates became extinct and only 2 of 8 replicate lines of the R12 homozygote population and 2 of 8 of the mixed population survived; in contrast, 7 of 8 HT strain replicates survived (HT versus Mix, HT versus R12 and HT versus G1; Fisher exact test P<0.04). In addition, the surviving HT populations were able to colonize more environments at the end of the experiment than those from the homozygote and mixed populations regardless of the treatment (Tukey HSD P<0.00005 after ANOVA effect of genotype on the number of colonized environments, F= 25.116, d.f.= 3, P<0.001).

Given the short duration of the selection experiment, new antibiotic resistance mutations arising in the populations are unlikely. Hence, our results strongly suggest that the better survival of the HT strain and its markedly improved ability to thrive in the range of environments after selection are a consequence of the preservation of allelic richness by

Europe PMC Funders Author Manuscripts

MCPs. Consistent with this view, we found that the HT strain maintained both alleles in a significantly higher number of environments than the mixed populations, both in constant regimes (35/181 versus 6/118 of colonized environments, respectively; χ^2= 11.088, d.f.= 1, P<0.001) and in fluctuating regimes (57/167 versus 1/35; χ^2= 12.341, d.f.= 1, P<0.001). Collectively, these results show that the maintenance of genetic diversity promoted by multicopy plasmids provides an evolutionary advantage in the colonization of new environments, especially when selective pressures rapidly shift.

Exploring the maintenance of plasmid-mediated heterozygosity under different selection regimes

A question that arises from our work is to what extent plasmid-mediated heterozygosity (PMH) can be maintained in bacterial populations. As the homozygotes or plasmid-free cells will eventually replace the HT strain in any possible constant environment, PMH is inherently unstable. However, PMH may be stabilized in dynamic environments that alternately select for each allele, as in drug cycling protocols23,24.

To test this possibility, we developed a simple compartmental population-dynamics model (Fig. 5) with parameter values obtained from experimental data (Methods and Supplementary table 3). Our model accurately reproduces the evolutionary dynamics that emerge from the interaction between heterozygote and homozygote populations competing for limiting resources and exposed to the action of Caz and Amp (Supplementary Figs. 6-7). By systematically exploring a range of fluctuating environmental regimes, we obtained relevant statistics about the population dynamics that arise as a consequence of different patterns of selection.

First, we considered treatments that alternate periodically between Caz and Amp at normalized drug dosages (by adjusting the concentration of each drug so that they achieve equal inhibitory effect). We simulated a range of concentrations and periods of cycling and computed, for each selection regime, the time elapsed until the density of HT cells is less than the initial bacterial density, a value we refer to as *duration of heterozygosity*. The realizations of the model showed that PMH can last for hundreds of days under regimes that present high frequencies of environmental switching and moderate drug concentrations (relative to the MIC of G1; Fig. 6).

However, fluctuations in nature are expected to be not periodic, but stochastic. To assess if the increased stability of PMH observed in periodic regimes is also present in stochastically-switching environments, we generated N=10,000 environmental regimes consisting of random sequences of both antibiotics. Each environmental regime is numerically generated by considering that the distribution of elapsed times between environmental switches follows an exponential distribution (see methods). We also evaluated environmental regimes that randomly switched between three discrete states (Caz, Amp and a drug-free environment) and obtained qualitatively the same results. The Shannon entropy25, H, of each previously determined environmental regime was used to quantify the uncertainty and stochasticity of each sequential treatment protocol. As shown in Fig. 6, environments with $H<<1$ have large single-drug time intervals that select for one of the homozygote strains and thus render PMH unstable. Conversely, duration of heterozygosity is maximized when

exposed to selection regimes associated with high entropy values and moderate selective pressures (Supplementary Fig. 8).

Together, our computational study predicts that heterozygosity can be stabilized for relatively long periods of time in fluctuating environments with high temporal heterogeneity and intermediate selective pressures.

Discussion

In this study, we investigated the role of MCPs in the alleviation of trade-offs during evolutionary innovation in bacteria. We developed a traceable model system using plasmid-mediated bla_{TEM} genes that reproduces the evolutionary dynamics toward Caz resistance21. Our results demonstrate that the intrinsic properties of replication and segregation dynamics of MCPs allow bacterial populations to escape the restraints imposed by trade-offs on the colonization of new environments by facilitating the co-existence of the ancestral and evolved alleles within the same cell (Fig. 2). Critically, this co-existence was maintained over tens of generations in the presence of increasingly strong pressures for the evolved allele (Fig. 3), suggesting that MCPs are able to delay the loss of non-adaptive allelic variants and preserve allelic richness for generations. Allelic richness, in turn, translates into increased phenotypic robustness to withstand stringent fluctuating selective pressures (Fig. 4). Collectively, our experimental and theoretical models establish that when the evolution of the plasmid resident loci is constrained by fitness trade-offs, the heterozygote has an advantage compared to the homozygotes. Hence, the population is under balancing selection for the maintenance of both ancestral and evolved alleles, especially when the environments fluctuate26. Although examples of selection favoring heterozygotes are abundant27,28, it comes as no surprise that these examples refer to polyploid eukaryotic organisms, in which new mutations are always heterozygous. In bacteria, MCP are able to provide heterozygote advantage because they represent an island of polyploidy in an otherwise haploid genome.

Previous studies have addressed the importance of MCPs in the evolution of new functions21,29,30, and the co-existence of mutant and ancestral allele variants encoded in the same plasmid has recently been demonstrated in laboratory evolution experiments21,31 and clinical settings32. However, the prevalence of plasmid-mediated heterozygosity in nature remains largely unknown. At least three arguments support the idea that plasmid-mediated heterozygosity could be pervasive in bacterial populations. First, natural MCPs encode important genes for bacterial physiology that are under strong selective forces such as antibiotic resistance genes33, determinants of ecological interactions such as colicins34, and even indispensable metabolic genes as in the aphid endosymbiont *Buchnera aphidicola*35. Second, MCPs are excellent platforms for the generation of genetic variation. Their multicopy nature increases the mutational supply and hence the chance of the resident loci acquiring mutations32. Additionally, this genetic variation can be further enriched by horizontal gene transfer18 and inter and intraplasmid recombination36,37. Third, MCPs are also excellent platforms for the preservation of genetic diversity. Our experimental results show that allelic richness can be maintained in the face of increasingly strong selective pressures for more than 75 bacterial generations, and our theoretical model indicates that it could be maintained for much longer periods under a range of conditions (Fig. 6 and

Supplementary figure 10). Considering that natural *E. coli* populations are estimated to undergo 100-300 generations per year38,39, we propose that the maintenance of genetic diversity by MCPs will persist long enough to profoundly affect bacterial evolvability. In view of these arguments, we predict that deep sequencing of bacterial clones (not populations) and careful examination of plasmid sequences from genomic data will increase the number of examples of plasmid-mediated heterozygosity in both experimental and natural scenarios.

Most plasmids cause a fitness cost to their host that should, in theory, constrain plasmid existence to very particular situations40,41. However, plasmids are extremely abundant in natural bacterial populations. This 'plasmid paradox' is particularly challenging in MCPs, as they lack mechanisms to increase their frequency such as active transfer or partitioning systems42. Several studies have offered compelling explanations for plasmid maintenance. For instance, epistatic interactions have been shown to buffer plasmid cost43,44. Moreover, this cost can be ameliorated by compensatory mutations in either the plasmid or the bacterial chromosome45–48. Other possible explanations involve the increase in gene copies for the resident loci, which in turn translates into increased gene expression that could be beneficial under certain circumstances21,35. Our results raise the possibility that MCPs, as promoters of bacterial evolution, could be maintained by second-order selection, a process by which evolution indirectly selects for the systems that create adaptive mutations49. We propose that while the conditions for the maintenance of plasmids by second-order selection will be stringent, they are plausible in bacterial populations49.

In conclusion, the ability of MCP-encoded genes to overcome the constraints imposed by trade-offs during evolutionary innovation could play a key role in the evolution of novel traits in bacterial populations and in the colonization of new environments. Additionally, our results may have implications for antibiotic therapies designed to slow the evolution of resistance by taking advantage of resistance trade-offs, such as drug cycling24 or the exploitation of collateral sensitivity networks50. Future work will be needed to test the extent to which MCPs can jeopardize the success of these promising antimicrobial strategies.

Methods

Strains, media and plasmid construction

The plasmids used in this study (Supplementary table 1) are derivatives of the pBGT and pBGT R164S plasmids that were previously used to reconstruct the plasmid-mediated evolution of Caz resistance21. For the sake of clarity, these plasmids were named pBGT-1 and pBGT-12 after the bla_{TEM} allele present. These plasmids also carry a *gfp* gene under the control of an L-arabinose inducible promoter, the gene coding for the repressor of this promoter *araC*, and a chloramphenicol (Chl) resistance acetyltransferase gene, *cat.* Variants of both plasmids in which the *gfp* gene was precisely replaced by the *dsRED* gene, encoding a red fluorescent protein, were generated by the Gibson assembly method51 using the primers listed in Supplementary table 2. To allow appropriate selection of heterozygote cells, a selective marker was needed to distinguish between plasmids. To this end, *cat* gene of the plasmids encoding $bla_{\mathrm{TEM\text{-}12}}$ was inactivated by creating an in-frame deletion (Δ574-591 in

cat ORF) by site-directed mutagenesis using the primers $Cat_{SDM}F$ and $Cat_{SDM}R$ (Supplementary table 2) and the Q5 Site-Directed Mutagenesis Kit (New England Biolabs) following manufacturer instructions. This deletion completely abolishes *cat* function by eliminating six essential aminoacids52 and renders the cells Chl sensitive. All possible combinations of the two bla_{TEM} alleles with both fluorescent markers were generated. All plasmids were introduced by transformation into chemically competent MG1655 cells giving rise to the strains shown in Supplementary table 1. Transformants were selected in Chl (15 mg/l) or Caz (1 mg/l) for plasmids carrying $bla_{TEM\text{-}1}$ and $bla_{TEM\text{-}12}$, respectively. To generate the heterozygote strains, two plasmids were simultaneously co-transformed and selected in both antibiotics. Transformants were checked by PCR using the primers listed in Supplementary table 2 and examined by confocal microscopy (Leica TCS SP5 multispectral confocal system) after induction of the fluorescent reporters by incubating the samples in LB supplemented with 0.1% L-arabinose during 4h. All strains were routinely grown in Lysogeny broth (LB) medium supplemented with the appropriate antibiotics at 37ºC.

In agreement with previous reports21, all plasmids-carriers showed a reduced growth rate compared to the plasmid-free strain although there were no significant differences among plasmid-bearing strains (Tukey's multiple comparison of means P>0.27; see Supplementary table 1). No significant differences in plasmid copy number (estimated by qPCR, see below) were found in the new constructs compared to G1 (Multiple comparisons of means, P>0.05), discarding any confounding effect in the interpretation of the data. Furthermore, genomic DNA of all the strains was isolated using the Wizard genomic DNA purification kit (Promega), following manufacturers' instructions. Whole genome sequencing was conducted at the Wellcome Trust Centre for Human Genetics using the Illumina HiSeq4000 platform. Possible mutations were predicted using the breseq 0.30.0 pipeline53 and using MG1655 genome (NC_000913.3) and plasmid sequences as references. Whole genome sequencing discarded the presence of unexpected mutations in coding regions of the chromosome or the plasmids in all the strains used in this study.

Antibiotic array

The antibiotic array was prepared in 96 well flat-bottom plates (Falcon) using the checkerboard technique54. To diminish inter-plate variability, all plates were prepared in the same day from a single stock solution using a Liquidator 96 Manual pipetting system (Mettler Toledo) and stored at -20ºC prior use. All plates were used within a week and appropriate controls were included to check antibiotic stability over time. Bacteria were inoculated at a final dilution of 1:2,000 and incubated during 20h at 37ºC. After incubation, optical density at 600nm (OD_{600}) was determined after strong shaking in a Synergy HTX microplate reader (Biotek). We interpreted that a particular environment of the array was colonized if, after incubation, OD_{600} was greater than 0.1. Appropriate samples were then collected to inoculate the next day plate. At the end of the experiment, plasmid DNA from samples of the surviving populations was extracted (Accuprep plasmid mini extraction kit; Bioneer) and the possible presence of plasmid hybrids containing both bla_{TEM} alleles was discarded by gel electrophoresis of undigested and Pvu*I* (New England Biolabs) digested plasmid extractions. To determine the fluorescence ratio (GFP/RFP), L-arabinose to a final concentration of 0.1% was added to each well to induce the expression of the fluorescent

reporters present on the plasmids. After 4h of incubation at 37ºC to allow protein expression, the plates were further incubated 18h at 4ºC. This step favors dsRED maturation, which is slower than that of GFP55. The GFP/RFP ratio was calculated by dividing green fluorescence (485/528 nm) over red fluorescence (540/590 nm) signals in a Synergy HTX microplate reader (Biotek). After collection of all data, GFP/RFP ratio was rescaled between 0.01 and 1 to make the results more amenable to interpretation.

Competition and invasion experiments

Minimal inhibitory concentrations (MIC) of Caz and Amp were determined for every strain by the microdilution method following CLSI guidelines56 (Supplementary table 1). Pairwise competitions between strains carrying $bla_{\text{TEM-1}}$ and $bla_{\text{TEM-12}}$ alleles were performed in media containing sub-inhibitory Caz concentrations and without antibiotics. Briefly, overnight cultures were mixed at 1:1 proportion and diluted 1:2,000 in fresh media. After 20h of incubation at 37ºC with shaking every 15 minutes in a Synergy HTX Multimode Reader (Biotek), appropriate dilutions were plated in LB agar plates containing Chl (15 mg/l) to select G1 and R1 strains or Caz (1 mg/l) to select G12 and R12 strains. The fitness of strains carrying $bla_{\text{TEM-12}}$ relative to the strains carrying $bla_{\text{TEM-1}}$ was determined using the formula:

$$W_{blaTEM12} = \frac{ln\left(N_{final;\,blaTEM12} \div N_{initial;\,blaTEM12}\right)}{ln\left(N_{final;\,blaTEM1} \div N_{initial;\,blaTEM1}\right)}$$

where $W_{\text{blaTEM-12}}$ is the relative fitness of the $bla_{\text{TEM-12}}$ bearing clone; $N_{\text{initial};bla\text{TEM-12}}$ and $N_{\text{final};bla\text{TEM-12}}$ are the numbers of $bla_{\text{TEM-12}}$ cells before and after the competition, and $N_{\text{initial};bla\text{TEM-1}}$ and $N_{\text{final};bla\text{TEM-1}}$ are the numbers of cells carrying $bla_{\text{TEM-1}}$ plasmids before and after the competition. The minimal selective concentration (MSC) of Caz, defined as the minimal antibiotic concentration that produces a detectable fitness benefit for the $bla_{\text{TEM-12}}$ carrying strains22, was used as starting concentration for the invasion experiments.

Invasion experiments were started by mixing overnight cultures of either HT or R12 and G1 strains at a 1:100 proportion in fresh LB. Immediately, the mixes were diluted 1:2,000 into 96 well flat-bottom plates (Falcon) containing 0.2ml of fresh media supplemented with the MSC of Caz. A checkerboard pattern was used to avoid cross-well contamination. After 20h of growth at 37ºC (approximately 11 bacterial generations per day), the cultures were further diluted 1:2,000 and inoculated into fresh media containing doubled antibiotic concentrations. Samples were plated in LB agar supplemented with either Caz (1 mg/l), Chl (15 mg/l) or Caz+Chl (1 mg/l+15 mg/l) to quantify the number of cells corresponding to each genotype in the competitions. To verify that the selective plating procedure was specific and to discard the presence of new mutations in the $bla_{\text{TEM-1}}$ gene, we sequenced the bla_{TEM} allele of four independent clones per replicate obtained on Caz+Chl plates at day 5 using the primers shown in Supplementary table 2. All chromatograms consistently showed a double peak (C+A) at the nucleotide 484 of the bla_{TEM} ORF assessing the presence of both $bla_{\text{TEM-1}}$ and $bla_{\text{TEM-12}}$ alleles in these clones. No other mutations were found. We

additionally ruled out the possible presence of plasmid hybrids containing both bla_{TEM} alleles by digestion as described above.

To assess allelic proportion, samples were also stored at -20ºC for subsequent qPCR analysis.

Quantification of plasmid copy number and allele frequencies

Quantitative polymerase chain reaction (qPCR) was used to determine relative plasmid copy number and allele frequency using an Applied Biosystems 7300 Real-Time PCR System and SYBR select master mix (Applied Biosystems). Specific primers for the pBGT plasmid backbone and the *dxs* chromosomal gene were used as previously described21. Additionally, specific primers for the *gfp* and *dsRED* genes were developed. All primer sequences can be found in Supplementary table 2. Samples were prepared as previously described57. Briefly, bacterial cultures were pelleted (9,000g, 1min), resuspended in molecular biology grade water and boiled (95ºC, 10min). After brief centrifugation to spin down cellular debris, samples of the supernatant were diluted and subsequently used as template. Amplification conditions were as follows: initial denaturation for 2 min at 95 °C, followed by 40 cycles of denaturation for 15 s at 95 °C, annealing and extension for 1 min at 60 °C. After the amplification was completed and to control for the specificity of the reaction, a melting curve analysis was performed by cooling the reaction to 60 °C and then heating slowly to 95 °C. Inter-run calibration samples were used to normalize the results from different plates of each qPCR. Relative copy number was calculated using the $\Delta\Delta C_T$ method as previously described58. All reactions showed similar efficiency values (92.7-93.8%, R^2>0.998) and produced amplicons of similar size (112-114bp). Control reactions were carried out to ensure that relative plasmid copy number was comparable when using pBGT or GFP and RFP targeting primers.

Calculation of Simpson's diversity index

When the relative abundance of each allele could be quantified by qPCR, Simpson's diversity index was used. Simpson's index gives the probability that two randomly selected alleles from the population are equal and can be calculated as $\sum\left(P^2_{blasTEM1} + P^2_{blaTEM12}\right)$ were P_i represents the relative proportion of each alelle59. Simpson's diversity index is an integrative measure that takes into account both population richness and evenness. In preliminary experiments, the GFP/RFP fluorescence ratio was found to strongly correlate with the allelic ratio estimated by qPCR (Pearson's product-moment correlation t =26.103, d.f. =16, R^2 =0.977, p $<10^{-13}$; Supplementary Fig. 5), demonstrating that it can be used as a proxy to assess the proportion of each allele. However, direct interpolation of allelic proportions from fluorescence data demonstrated to be unreliable. Instead, we used a more conservative approach in which the presence of both alleles in a particular environment was assessed by simply determining if the GFP/RFP ratio was comprised between that of the homozygotes. In this way, allelic richness of an environment can be confidently determined. We note, however, that this method underestimates the real environmental richness as populations carrying a small number of one plasmid type would show undetectable levels of fluorescence. In that sense, for an environment to be classified as having both alleles, it must have substantial amounts of both plasmids. We argue that this is indeed a strength of this

approach, because an environment must show some extent of allelic evenness to be cataloged as rich by our method.

Population-level plasmid dynamics model

The objective of our model is to study the population dynamics that emerges in response to different environmental concentrations of resource and multiple bactericidal antibiotics. First, we will assume that the bacterial population is composed of a plasmid-free subpopulation (with density at time t denoted by $B_{PF}(t)$), a subpopulation of heterozygote cells (with density represented by $B_{HT}(t)$) and homozygote subpopulations G1 and R12 (with densities represented with $B_{G1}(t)$ and $B_{R12}(t)$, respectively). We will consider that growth of each subpopulation depends on the environmental concentration of a limiting resource, $R(t)$, and therefore we can model growth rate of subpopulation i with a standard Monod term, $G_i(R(t)) = \rho_i U_i(R(t))$, where ρ_i is the metabolic efficiency of the cell and $U_i(R) = V_i R/(K_i + R)$ a sigmoidal resource uptake function characterized by parameters V_i and K_i denoting, respectively, the maximum growth rate and half-saturation constants of bacterial type i. In order to model the action of antibiotics (in this case drugs Amp and Caz, with an additive interaction and concentration represented by D^A and D^C respectively) we consider that the susceptibility of strain B_i to Amp and Caz can be modeled with killing rates κ_i^A and κ_i^C. Conversely, δ_i^A and δ_i^C denote the rates of drug inactivation by the degrading enzyme produced by bacterial type i.

Note that the plasmids used in this study replicate as monomers and do not possess any molecular mechanisms that increase its stability (e.g. active partitioning or post-segregational killing mechanisms). Therefore, we can assume that plasmids are uniformly distributed in the cell at the moment of division and, as a result, the probability of a plasmid-bearing cell producing a plasmid-free cell through segregation can be described by a Poisson process and thus the rate of plasmid loss via segregation is approximated by $\Sigma = 2^{1-\mu}$, where μ denotes the mean plasmid copy number in the population47,60. Similarly, the probability of a heterozygote cell giving rise to a homozygote cell can be estimated by assuming that, in average, HT cells have equal fractions of both plasmids and thus the rate of heterozygosity loss can be written as $\sigma = 2^{1-\mu/2}$. Therefore, our model makes the critical assumption that HT cells carry equal proportions of each plasmid. Although this simplification may underestimate the complex distribution of intracellular allele frequencies, our model accurately reproduces the experimental results (Supplementary Fig. 6 and 7). In our experimental system, the mean per-cell plasmid copy number is 19 and therefore the rate of heterozygosity loss is 1/362 while the rate of plasmid loss is considerably lower, at 1/524,288. Finally, the evolutionary dynamics of the system considers that the transition from B_{G1} and B_{R12} into B_{HT} occurs at a rate $\varepsilon > 0$ representing the probability of a single-point mutation in the $bla_{\text{TEM-1}}$ or $bla_{\text{TEM-12}}$ locus.

In summary, the system of ordinary differential equations that describe the plasmid dynamics at a population-level can be written as:

(1) $$\frac{d}{dt}R = -\left(U_{PF}(R)B_{PF} + U_{G1}(R)B_{G1} + U_{HT}(R)B_{HT} + U_{R12}(R)B_{R12}\right)$$

(2) $$\frac{d}{dt}D^A = -D^A\left(\delta^A_{PF}B_{PF} + \delta^A_{G1}B_{G1} + \delta^A_{HT}B_{HT} + \delta^A_{R12}B_{R12}\right)$$

(3) $$\frac{d}{dt}D^C = -D^C\left(\delta^C_{PF}B_{PF} + \delta^C_{G1}B_{G1} + \delta^C_{HT}B_{HT} + \delta^C_{R12}B_{R12}\right)$$

(4) $$\frac{d}{dt}B_{PF} = G_{PF}(R)B_{PF} + \Sigma\left(G_{G1}(R)B_{G1} + G_{HT}(R)B_{HT} + G_{R12}(R)B_{R12}\right) - B_{PF}(\kappa^A_{PF}D^A + \kappa^C_{PF}D^C)$$

(5) $$\frac{d}{dt}B_{G1} = (1-\varepsilon-\Sigma)G_{G1}(R)B_{G1} + \sigma G_{HT}(R)B_{HT} - B_{G1}(\kappa^A_{G1}D^A + \kappa^C_{G1}D^C)$$

(6) $$\frac{d}{dt}B_{HT} = (1-\Sigma)G_{HT}(R)B_{HT} + \varepsilon(G_{G1}(R)B_{G1} + G_{R12}(R)B_{R12}) - B_{HT}(\kappa^A_{HT}D^A + \kappa^C_{HT}D^C)$$

(7) $$\frac{d}{dt}B_{R12} = (1-\varepsilon-\Sigma)G_{R12}(R)B_{R12} + \sigma G_{HT}B_{HT} - B_{R12}(\kappa^A_{R12}D^A + \kappa^C_{R12}D^C)$$

with parameters values estimated using a parametrization approach that implements a Markov Chain Monte Carlo (MCMC) method with Metropolis-Hastings sampling. A similar Bayesian approach was published previously47 and allows us to obtain maximum likelihood estimates for the specific affinity V_i/K_i and the resource conversion rate, ρ_i, from experimental growth curves of each strain grown in isolation (Supplementary Fig. 9 shows the MCMC diagnostics plots). The inhibition parameters of each strain were estimated using single-drug dose-response experiments. Numerical solutions of the system of equations (1-7) were obtained using standard ODE solvers in Matlab, with parameter values summarized in Supplementary table 3.

Computational experiments in fluctuating environments

In order to numerically simulate an N-day experimental serial dilution protocol, we considered that each day ($0 \leq n < N$) resources are replenished at the beginning of each season, that is $R_n(0) = R_0$. The initial bacterial density on the first day ($n = 0$) can be written as $B_0 \cdot \Gamma$, where $B_0 = 1\times10^6$ denotes the total initial bacterial density and $\Gamma = (\gamma_{PF}, \gamma_{G1}, \gamma_{HT}, \gamma_{R12})$ a vector containing the initial relative frequencies of each strain and thus $\gamma_{PF} + \gamma_{G1} + \gamma_{HT} + \gamma_{R12} = 1$. For subsequent seasons, $n > 1$, we consider the initial population density of each subpopulation to be a function of the terminal condition of the previous season, that is $\eta \cdot (B_{PF}(T), B_{G1}(T), B_{HT}(T), B_{R12}(T))$, whereby $\eta = 0.01$ denotes the dilution parameter and $T = 24$ the duration of each season.

To quantify the stability of single-cell genetic diversity, we use the duration of heterozygosity, τ, defined as the time elapsed until the density of B_{HT} is below an extinction threshold, that is $\tau > 0$ such that $B_{HT}(\tau) < B_{ext} = 1\times10^6$ and $B_{HT}(t) \geq B_{ext}$ for all $t \in$. In particular, we considered fluctuating environmental regimes that alternate selection between both drugs, so if $\hat{D}^A$ and $\hat{D}^C$, represent the concentrations of each drug normalized to achieve equal inhibitory effect then on day n we can represent the treatment used as $D_n = \phi_n\hat{D}^A + (1-\phi_n)\hat{D}^C$. Here, we used $\phi_n = 0$ or $\phi_n = 1$ and therefore the environmental regime could be represented as a random sequence of N bits, allowing us to compute the information entropy (Shannon-Wiener Index) associated with each environmental sequence

using the following expression: $H = -\sum\left(P \cdot log_2(P)\right)$ where P represents the proportion of days where each drug was used. Note that low-values of H correspond to constant, predictable environments, while high entropy values are associated with unpredictable, rapidly-switching environmental conditions.

The bla TEM-1 /bla TEM-12 trade-off explored in this work can be considered “weak” in the sense that the gain in the new function is big (64 fold increase in Caz MIC), whereas the loss in the ancestral function is small (2 fold reduction in Amp MIC). In natural and laboratory evolution most trade-offs are weak2 (> 10 fold gain in new function versus loss of the existing one) and hence the trade-off of TEM evolution used in this work can be deemed representative. Nevertheless, we decided to theoretically explore various trade-off strengths to extend our computational analysis to other possible scenarios. As can be seen in Supplementary figure 10, stronger trade-offs increase the range of fluctuations and antibiotic pressures that render PMH stable. In contrast weaker trade-offs render PMH unstable in most conditions, as the acquisition of a new genetic activity barely involves any loss in the ancestral function.

Statistical analysis

Analyses were performed using R (Version 3.4.2)61. One way ANOVA and Tukey's multiple comparison of means were used to assess differences in colonization in the antibiotic array. Spearman's rank correlation coefficient was used to assess the monotonic relationship between antibiotic concentrations and the GFP/RFP ratio. Chi-squared (χ^2) test was used to analyze the frequency of populations conserving both alleles after growth in the antibiotic array. Repeated-Measures ANOVA was used to ascertain the variation of Simpson allelic diversity index over time in the invasion experiments. Fisher's exact test was used to analyze the differences in survival in the short-term selection experiment. Two-tailed two-sample *t*-test with Bonferroni correction were used to compare fitness data. Pearson's product-moment correlation was used to assess the linear relationship between fluorescence and plasmid proportion determined by qPCR.

Data availability

The sequence data that support the findings of this study have been deposited in the European Nucleotide Archive with the accession code PRJEB25055 (http://www.ebi.ac.uk/ena/data/view/PRJEB25055)

Supplementary Material

Refer to Web version on PubMed Central for supplementary material.

Acknowledgments

We thank R. León-Sampedro for valuable technical assistance with bioinformatic analyses. This work was supported by the Instituto de Salud Carlos III (Plan Estatal de I+D+i 2013-2016): grants CP15-00012, PI16-00860, and CIBER (CB06/02/0053), co-financed by the European Development Regional Fund “A way to achieve Europe” (ERDF). R.P.M and R.C.M are supported by a Newton Advanced Fellowship awarded by the Royal Society (NA140196). R.P.M and A.F.H are funded by UNAM-PAPIIT (IA201017 & IA201016). R.C.M was supported by a Wellcome Trust Senior Research Fellowship (WT106918AIA). J.C.R.H is a doctoral student from Programa de Doctorado en Ciencias Biomédicas, Universidad Nacional Autónoma de México (UNAM) and received fellowship

596191 from CONACYT. J.A.E. is supported by the Atracción de Talento program of the Comunidad de Madrid (2016-T1/BIO-1105). A.S.M is supported by a Miguel Servet Fellowship from the Instituto de Salud Carlos III (MS15/00012) cofinanced by The European Social Fund "Investing in your future" (ESF) and ERDF.

References

1. Conant GC, Wolfe KH. Turning a hobby into a job: how duplicated genes find new functions. Nat Rev Genet. 2008; 9:938–50. [PubMed: 19015656]
2. Khersonsky O, Tawfik DS. Enzyme promiscuity: a mechanistic and evolutionary perspective. Annu Rev Biochem. 2010; 79:471–505. [PubMed: 20235827]
3. Toll-Riera M, San Millan A, Wagner A, MacLean RC. The Genomic Basis of Evolutionary Innovation in Pseudomonas aeruginosa. PLoS Genet. 2016; 12:1–21.
4. Childers WS, et al. Cell Fate Regulation Governed by a Repurposed Bacterial Histidine Kinase. PLoS Biol. 2014; 12:e1001979. [PubMed: 25349992]
5. Anderson DP, et al. Evolution of an ancient protein function involved in organized multicellularity in animals. Elife. 2016; 5:e10147. [PubMed: 26740169]
6. Bershtein S, Tawfik DS. Ohno's model revisited: Measuring the frequency of potentially adaptive mutations under various mutational drifts. Mol Biol Evol. 2008; 25:2311–2318. [PubMed: 18687656]
7. Stiffler MA, Hekstra DR, Ranganathan R. Evolvability as a Function of Purifying Selection in TEM-1 β-Lactamase. Cell. 2015; 160:882–892. [PubMed: 25723163]
8. Soskine M, Tawfik DS. Mutational effects and the evolution of new protein functions. Nat Rev Genet. 2010; 11:572–582. [PubMed: 20634811]
9. Innan H, Kondrashov F. The evolution of gene duplications: classifying and distinguishing between models. Nat Rev Genet. 2010; 11:97–108. [PubMed: 20051986]
10. Andersson DI, Hughes D. Gene amplification and adaptive evolution in bacteria. Annu Rev Genet. 2009; 43:167–195. [PubMed: 19686082]
11. Bergthorsson U, Andersson DI, Roth JR. Ohno's dilemma: evolution of new genes under continuous selection. Proc Natl Acad Sci U S A. 2007; 104:17004–17009. [PubMed: 17942681]
12. Pettersson ME, Sun S, Andersson DI, Berg OG. Evolution of new gene functions: simulation and analysis of the amplification model. Genetica. 2009; 135:309–324. [PubMed: 18568430]
13. Adler M, Anjum M, Berg OG, Andersson DI, Sandegren L. High Fitness Costs and Instability of Gene Duplications Reduce Rates of Evolution of New Genes by Duplication-Divergence Mechanisms. Mol Biol Evol. 2014; 31:1526–1535. [PubMed: 24659815]
14. Sandegren L, Andersson DI. Bacterial gene amplification: implications for the evolution of antibiotic resistance. Nat Rev Microbiol. 2009; 7:578–588. [PubMed: 19609259]
15. Toussaint J-P, et al. Gene Duplication in Pseudomonas aeruginosa Improves Growth on Adenosine. J Bacteriol. 2017; 199:e00261–17. [PubMed: 28808129]
16. Näsvall J, Sun L, Roth JR, Andersson DI. Real-Time Evolution of New Genes by Innovation, Amplification, and Divergence. Science (80-.). 2012; 338
17. Stoesser N, et al. Evolutionary History of the Global Emergence of the Escherichia coli Epidemic Clone ST131. MBio. 2016; 7:e02162. [PubMed: 27006459]
18. SummersDK. The Biology of PlasmidsBlackwell Publishing Ltd.; 2009
19. Mroczkowska JE, Barlow M. Fitness trade-offs in blaTEM evolution. Antimicrob Agents Chemother. 2008; 52:2340–2345. [PubMed: 18443128]
20. Schenk MF, et al. Role of pleiotropy during adaptation of TEM-1 B-lactamase to two novel antibiotics. Evol Appl. 2015; 8:248–260. [PubMed: 25861383]
21. San Millan A, Escudero JA, Gifford DR, Mazel D, MacLean RC. Multicopy plasmids potentiate the evolution of antibiotic resistance in bacteria. Nat Ecol Evol. 2016; 1:10. [PubMed: 28812563]
22. Gullberg E, et al. Selection of resistant bacteria at very low antibiotic concentrations. PLoS Pathog. 2011; 7:e1002158. [PubMed: 21811410]
23. Fuentes-Hernandez A, et al. Using a Sequential Regimen to Eliminate Bacteria at Sublethal Antibiotic Dosages. PLOS Biol. 2015; 13:e1002104. [PubMed: 25853342]

24. Kim S, Lieberman TD, Kishony R. Alternating antibiotic treatments constrain evolutionary paths to multidrug resistance. Proc Natl Acad Sci. 2014; 111:14494–14499. [PubMed: 25246554]
25. Shannon CE. A Mathematical Theory of Communication. Bell Syst Tech J. 1948; 27:623–656.
26. Charlesworth D. Balancing selection and its effects on sequences in nearby genome regions. PLoS Genetics. 2006; 2:379–384.
27. Sellis D, Kvitek DJ, Dunn B, Sherlock G, Petrov DA. Heterozygote Advantage Is a Common Outcome of Adaptation in Saccharomyces cerevisiae. Genetics. 2016; 203:1401–13. [PubMed: 27194750]
28. Niskanen AK, et al. Balancing selection and heterozygote advantage in major histocompatibility complex loci of the bottlenecked Finnish wolf population. Mol Ecol. 2014; 23:875–889. [PubMed: 24382313]
29. Holloway AK, Palzkill T, Bull JJ. Experimental evolution of gene duplicates in a bacterial plasmid model. J Mol Evol. 2007; 64:215–222. [PubMed: 17211548]
30. Dhar R, Bergmiller T, Wagner A. Increased gene dosage plays a predominant role in the initial stages of evolution of duplicate tem-1 beta lactamase genes. Evolution (N. Y). 2014; 68:1775–1791.
31. Bedhomme S, Perez Pantoja D, Bravo IG. Plasmid and clonal interference during post horizontal gene transfer evolution. Mol Ecol. 2017; 26:1832–1847. [PubMed: 28206693]
32. Santos-Lopez A, et al. A naturally occurring SNP in plasmid pB1000 produces a reversible increase in antibiotic resistance. Antimicrob Agents Chemother. 2016; 2 AAC.01735-16.
33. Wu PJ, Shannon K, Phillips I. Mechanisms of hyperproduction of TEM-1 beta-lactamase by clinical isolates of Escherichia coli. J Antimicrob Chemother. 1995; 36:927–39. [PubMed: 8821592]
34. Cascales E, et al. Colicin biology. Microbiol Mol Biol Rev. 2007; 71:158–229. [PubMed: 17347522]
35. Latorre A, Gil R, Silva FJ, Moya A. Chromosomal stasis versus plasmid plasticity in aphid endosymbiont Buchnera aphidicola. Heredity (Edinb). 2005; 95:339–347. [PubMed: 16118664]
36. Gomez A, et al. Creating new genes by plasmid recombination in Escherichia coli and Bacillus subtilis. Appl Environ Microbiol. 2005; 71:7607–9. [PubMed: 16269814]
37. Rodríguez-Beltrán J, et al. High Recombinant Frequency in Extraintestinal Pathogenic Escherichia coli Strains. Mol Biol Evol. 2015; 32:1708–1716. [PubMed: 25804522]
38. Guttman DS, Dykhuizen DE. Clonal divergence in Escherichia coli as a result of recombination, not mutation. Science (80-.). 1994; 266:1380–3.
39. Gibbons RJ, Kapsimalis B. Estimates of the overall rate of growth of the intestinal microflora of hamsters, guinea pigs, and mice. J Bacteriol. 1967; 93:510–2. [PubMed: 6020422]
40. Vogwill T, Maclean RC. The genetic basis of the fitness costs of antimicrobial resistance: A meta-analysis approach. Evol Appl. 2015; 8:284–295. [PubMed: 25861386]
41. San Millan A, MacLean RC. Fitness Costs of Plasmids: a Limit to Plasmid Transmission. Microbiol Spectr. 2017; 5
42. Smillie C, Garcillán-Barcia MP, Francia MV, Rocha EPC, de la Cruz F. Mobility of plasmids. Microbiol Mol Biol Rev. 2010; 74:434–52. [PubMed: 20805406]
43. San Millan A, Heilbron K, MacLean RC. Positive epistasis between co-infecting plasmids promotes plasmid survival in bacterial populations. ISME J. 2014; 8:601–612. [PubMed: 24152711]
44. Silva RF, et al. Pervasive sign epistasis between conjugative plasmids and Drug-Resistance chromosomal mutations. PLoS Genet. 2011; 7:e1002181. [PubMed: 21829372]
45. Harrison E, et al. Parallel Compensatory Evolution Stabilizes Plasmids across the Parasitism-Mutualism Continuum Current Biology Report Parallel Compensatory Evolution Stabilizes Plasmids across the Parasitism-Mutualism Continuum. Curr Biol. 2015; 25:2034–2039. [PubMed: 26190075]
46. Porse A, Schønning K, Munck C, Somme MOA. Survival and Evolution of a Large Multidrug Resistance Plasmid in New Clinical Bacterial Hosts. Mol Biol Evol. 2016; 33:2860–2873. [PubMed: 27501945]

47. San Millan A, et al. Positive selection and compensatory adaptation interact to stabilize non-transmissible plasmids. Nat Commun. 2014; 5:5208. [PubMed: 25302567]
48. Loftie-Eaton W, et al. Compensatory mutations improve general permissiveness to antibiotic resistance plasmids. Nat Ecol Evol. 2017; 1:1354–1363. [PubMed: 29046540]
49. Tenaillon O, Taddei F, Radman M, Matic I. Second-order selection in bacterial evolution: Selection acting on mutation and recombination rates in the course of adaptation. Research in Microbiology. 2001; 152:11–16. [PubMed: 11281320]
50. Imamovic L, Sommer MOA. Use of Collateral Sensitivity Networks to Design Drug Cycling Protocols That Avoid Resistance Development. Sci Transl Med. 2013; 5:204ra132–204ra132.
51. Gibson DG, et al. Enzymatic assembly of DNA molecules up to several hundred kilobases. Nat Methods. 2009; 6:343–345. [PubMed: 19363495]
52. Leslie AG, Moody PC, Shaw WV. Structure of chloramphenicol acetyltransferase at 1.75-A resolution. Proc Natl Acad Sci U S A. 1988; 85:4133–4137. [PubMed: 3288984]
53. Deatherage DE, Barrick JE. Identification of mutations in laboratory-evolved microbes from next-generation sequencing data using breseq. Methods Mol Biol. 2014; 1151:165–88. [PubMed: 24838886]
54. Bonapace CR, Bosso JA, Friedrich LV, White RL. Comparison of methods of interpretation of checkerboard synergy testing. Diagn Microbiol Infect Dis. 2002; 44:363–366. [PubMed: 12543542]
55. Gross LA, Baird GS, Hoffman RC, Baldridge KK, Tsien RY. The structure of the chromophore within DsRed, a red fluorescent protein from coral. Proc Natl Acad Sci. 2000; 97:11990–11995. [PubMed: 11050230]
56. CLSI. Performance Standards for Antimicrobial Susceptibility Testing; Twenty-Second Informational Supplement. Clin Lab Stand Inst. 2014; 34:1–219.
57. Skulj M, et al. Improved determination of plasmid copy number using quantitative real-time PCR for monitoring fermentation processes. Microb Cell Fact. 2008; 7:6. [PubMed: 18328094]
58. Livak KJ, Schmittgen TD. Analysis of Relative Gene Expression Data Using Real-Time Quantitative PCR and the 2−ΔΔCT Method. Methods. 2001; 25:402–408. [PubMed: 11846609]
59. Jost L. Entropy and diversity. Oikos. 2006; 113:363–375.
60. Summers DK. The kinetics of plasmid loss. Trends Biotechnol. 1991; 9:273–8. [PubMed: 1367567]
61. R Core Team. R: A Language and Environment for Statistical Computing. 2017
62. Levin BR, Stewart FM. The population biology of bacterial plasmids: a priori conditions for the existence of mobilizable nonconjugative factors. Genetics. 1980; 94:425–443. [PubMed: 6248416]

Europe PMC Funders Author Manuscripts

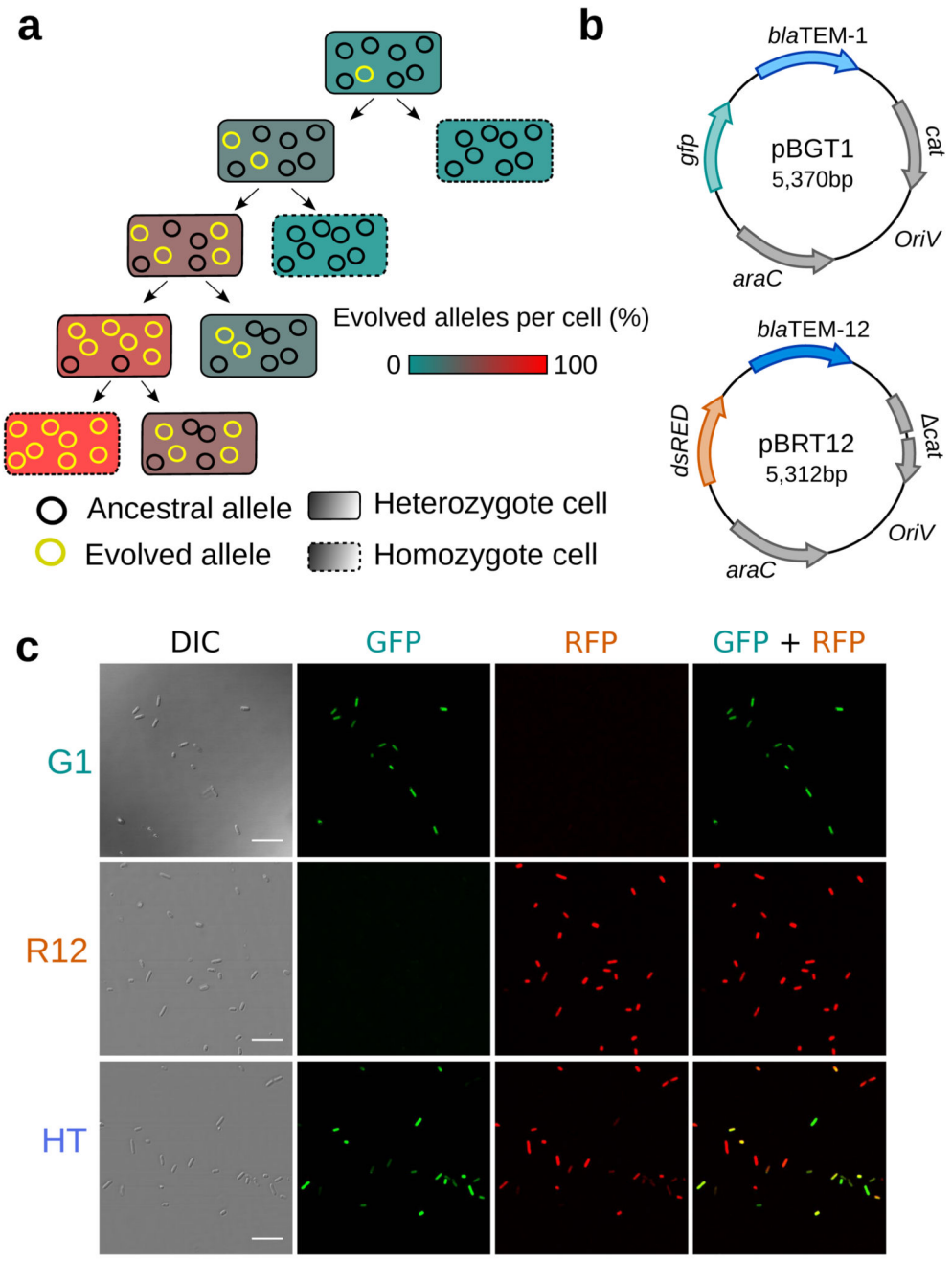

Figure 1. Conceptual and experimental models.

(**a**) Scheme of the plasmid replication and segregation dynamics that drive the co-existence of ancestral and mutated alleles under heterozygosity. In every generation, plasmids are randomly segregated to daughter cells and then replicated. Following this simple model, heterozygosity is maintained for several generations as an emergent property of plasmid replication and segregation dynamics. (**b**) Maps of the plasmids used in our experimental model. (**c**) Confocal microscopy images showing representative fields of bacterial populations of the G1 and R12 homozygote strains, and the HT strain. Scale bar, 10 μm.

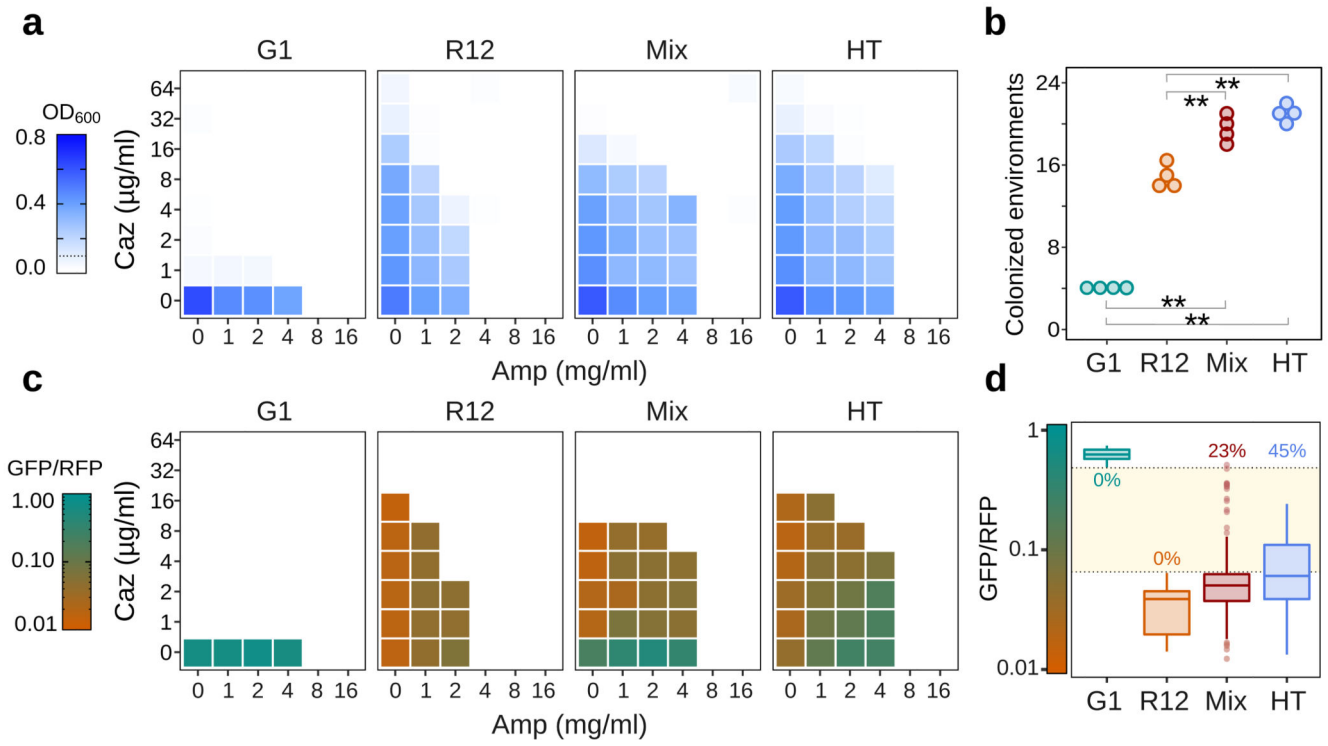

Figure 2. Bacterial growth and allelic content in the antibiotics array.

(**a**) The optical density (OD_{600}) of populations growing in a range of concentrations of Caz and Amp alone or in combination is color-coded as indicated in the legend. We concluded that a particular environment in the array was colonized if, after 20h of incubation, OD_{600} was greater than 0.1 (dashed line in the legend). (**b**) The number of colonized environments of the four replicate arrays plotted for every genotype and the mixed population. The asterisks denote significant differences (Tukey test $P<0.001$ after significant ANOVA). (**c**) The GFP/RFP fluorescence ratio (arbitrary units) offers insight into the allelic content of every environment and is plotted according the color code shown in the legend. (**d**) Boxplots showing the distribution of fluorescence ratios in four replicate arrays for each genotype. The yellow-shaded region denotes fluorescence levels between those of the G1 and R12 strains and thus those populations carrying both plasmids at detectable levels. The numbers designate the percentage of environments colonized by a population containing both plasmids. For the sake of clarity only one of four replicates is shown in **a** and **c**. All four individual replicates can be found in Supplementary Data 1, under the label “day 1”.

Europe PMC Funders Author Manuscripts

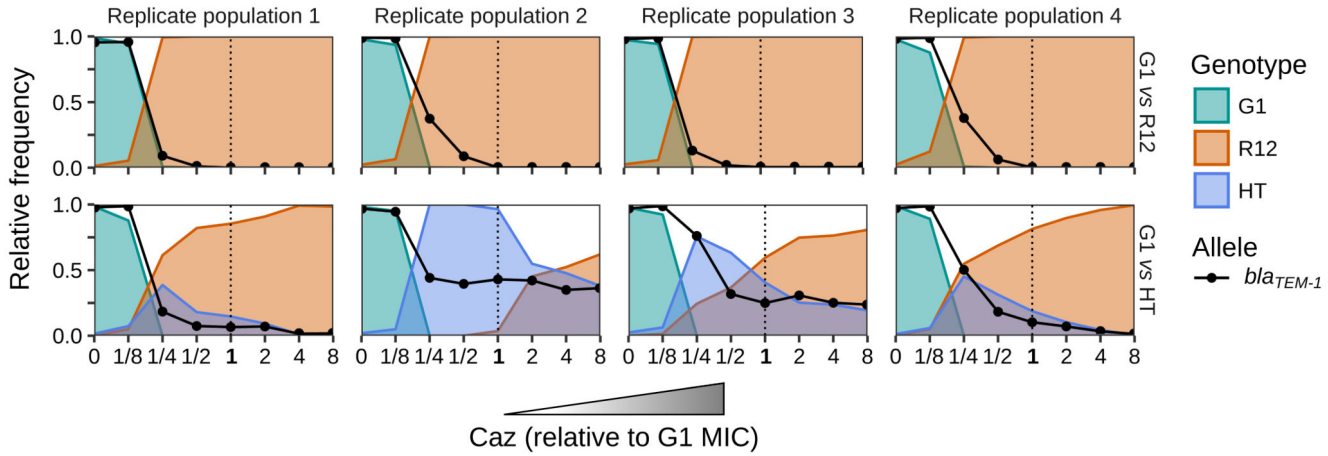

Figure 3. Invasion experiments.

The upper panels show invasion experiments in which G1 population was invaded by a rare R12 population (1%); the lower panels show invasion experiments in which the HT strain invaded instead of R12. Experimental results obtained with four replicate populations (columns). Invasion experiments were carried out eight consecutive days in which the Caz concentration in the medium was doubled daily. Each panel shows, for an individual invasion, the relative frequency of every genotype on each day, calculated by selective plating (filled areas). The solid black line shows the frequency of pBGT-1/pBRT-12 ($bla_{\text{TEM-1}}/bla_{\text{TEM-12}}$) calculated by qPCR. The black dashed vertical line denotes the day on which the MIC of Caz for G1 was reached.

Europe PMC Funders Author Manuscripts

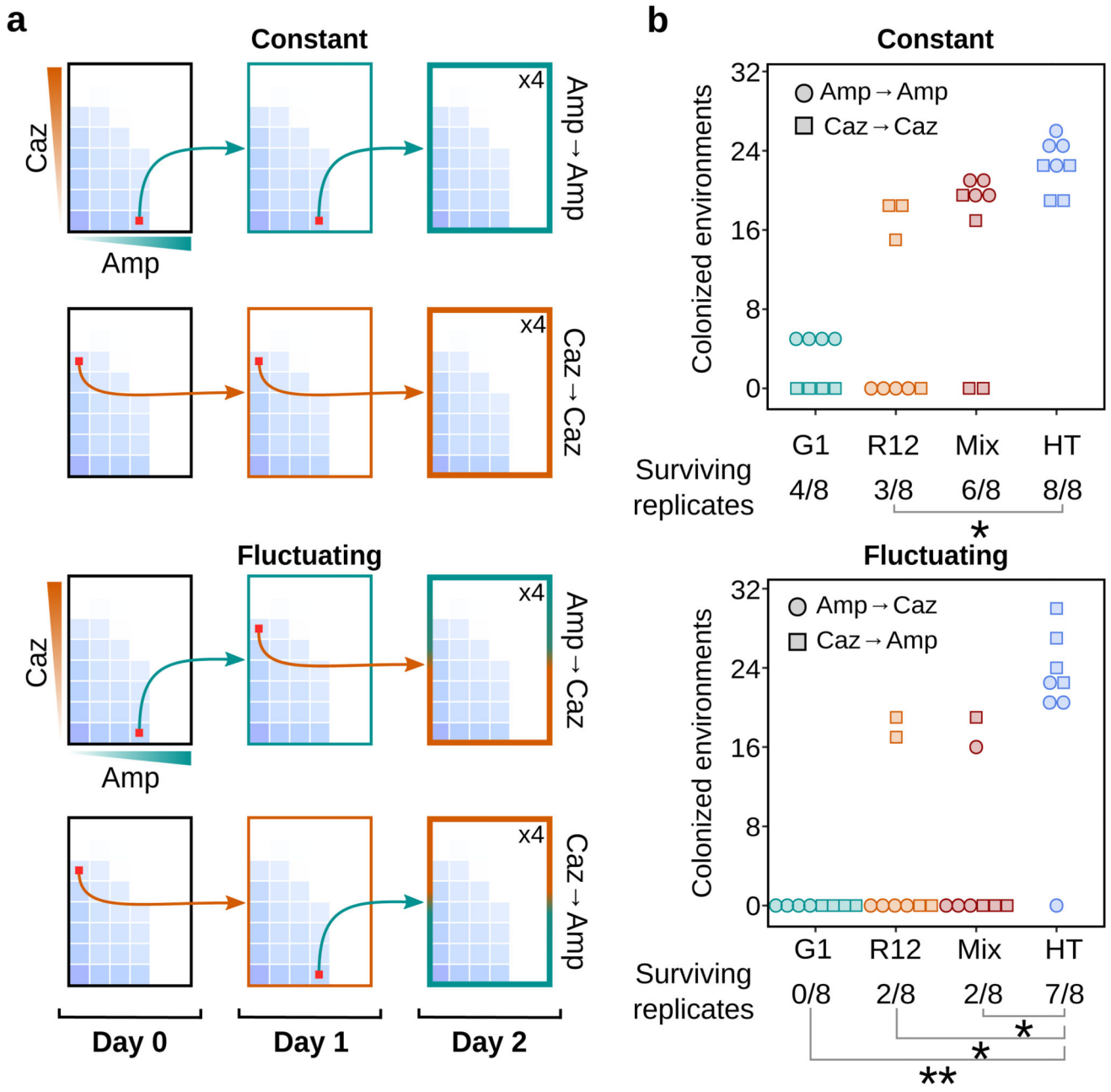

Figure 4. MCPs alleviate trade-offs under strong selective pressures.

(**a**) Experimental design. Each plate represents an antibiotic array (identical to those shown in figure 2) from which the bacterial populations growing in either high Caz or high Amp concentrations (red filled squares) were diluted and used to sequentially seed new antibiotic arrays over a two day course. This gives rise to four selective regimes; two in which selection was held constant (Caz→Caz and Amp→Amp) and two with fluctuating selection (Caz→Amp and Amp→Caz). **(b)** Dot plot showing the number of colonized environments by each replicate line at the end of the experiment (day two). Each dot represents a replicate line, and the symbol denotes the antibiotic treatment. Populations that became extinct

colonized zero environments. Note that the results are grouped by the type of selection regimen. Under each panel, the number of surviving replicates is shown together with asterisks denoting statistical significance (* $P<0.05$, ** $P<0.002$; χ^2 test). Raw data of all replicates can be found in the Supplementary Data 1.

Europe PMC Funders Author Manuscripts

Europe PMC Funders Author Manuscripts

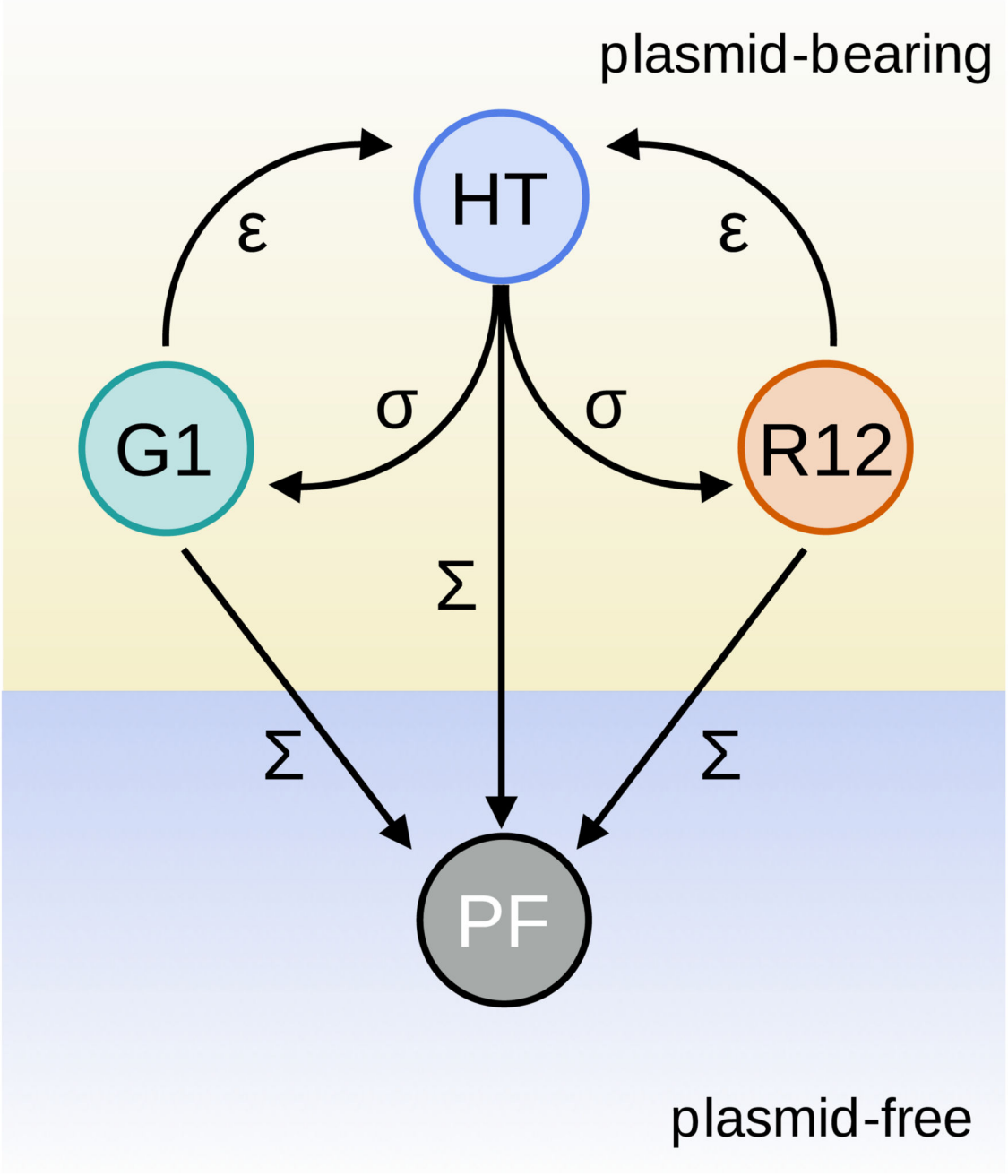

Figure 5. Theoretical model.

Diagram illustrating the population dynamics of homozygote cells (G1 and R12), heterozygote cells (HT) and plasmid-free cells (PF). As described in the methods section, we assume that plasmids are uniformly distributed in the cell and therefore the rate of segregational loss (Σ) can be derived from the population-level mean plasmid copy number (see Methods and62). Transitions between HT to G1 and R12 are also segregation-driven processes that occur at a rate σ, a parameter that can be estimated by assuming that HT cells

have, in average, equal allelic proportions. The HT cells are produced by single-point mutation (occurring at a rate ε) in either G1 or R12 strains.

Europe PMC Funders Author Manuscripts

Europe PMC Funders Author Manuscripts

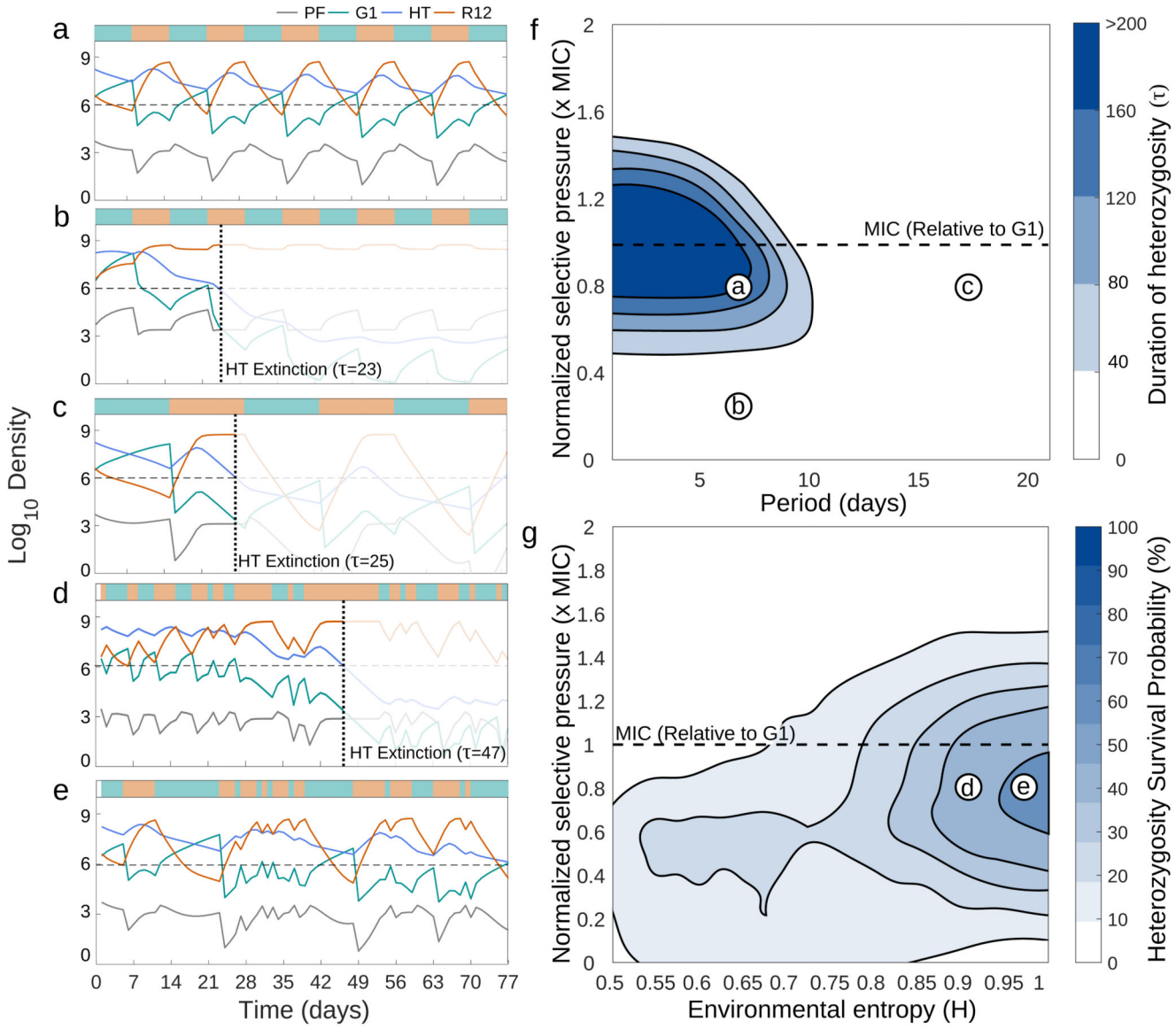

Figure 6. Numerical examples predicting the duration of plasmid-mediated heterozygosity under a range of fluctuating antibiotic conditions.

(**a-c**) Population dynamics in response to periodic selection regimes annotated in (**f**). For clarity, only the densities at the end of each day are shown. (**d-e**) Realizations of the model under the specific stochastic selection regimes annotated in (**g**). (**f**) Heat map representing the duration of heterozygosity under a range of normalized drug concentrations and periods of alternating drug exposure. Note how the regime *a* deploys drugs at 0.8xMIC in a 7-day period and is able to maintain the density of HT above the extinction threshold (in this case 10^6 cells). However, if the dose (as in regime *b*) or the frequency of environmental switching (as in regime *c*) is reduced, then the HT subpopulation is driven towards extinction. (**g**) Heat map representing the survival probability of the HT population in response to different

antibiotic concentrations and the entropy of the environment, a property that represents the uncertainty of each sequential treatment protocol.

Europe PMC Funders Author Manuscripts